Polym. Bull. (2013) 70:3103–3113
DOI 10.1007/s00289-013-1010-4

ORIGINAL PAPER

Cu nanoparticles for improving the mechanical performances of oil palm empty fruit bunch fibers as analyzed by Weibull model

M. N. K. Chowdhury · M. F. Mina · M. D. H. Beg · Maksudur R. Khan

Received: 27 April 2013 / Accepted: 1 August 2013 / Published online: 15 August 2013

Abstract Cu nanoparticles (CuNPs) were impregnated in oil palm empty fruit bunch (EFB) fibers via the cationization process. The fiber surface modification by CuNPs has been verified by Fourier-transformed infrared spectroscopy, field emission scanning electron microscopy and energy dispersive X-ray study. Mechanical properties were measured by the tensile test and analyzed by the Griffith and the Weibull models. The 10 mm length EFB fiber modified by CuNPs shows an increment in characteristic strength (σ_0) and modulus (Y_0) by about 20 and 10 % compared to the unmodified fiber, as assessed by the Weibull model. This improvement in mechanical properties is associated with the incorporation of CuNPs in the fibers. Weak-link scaling model has been applied to predict the mechanical properties of unknown fiber.

Keywords Nanoparticles · Natural fibers · Mechanical properties · Weibull model

Introduction

Nowadays, cellulosic fiber has gained importance to meet up the demand of environment friendly, low-cost and biocompatible products in composites, medical supplies, textiles, packaging, energy storage, electronic devices and biomedical materials [1–4]. Despite their usage in several fields, cellulosic fiber cannot be potentially utilized in versatile applications due to its high hydrophilic nature, poor mechanical strength, and no antimicrobial activity [5]. In spite of high content of cellulose (43–65 %) [6], oil palm empty fruit bunch (EFB)

M. N. K. Chowdhury · M. F. Mina · M. D. H. Beg · M. R. Khan (✉)
Faculty of Chemical and Natural Resources Engineering, Universiti Malaysia Pahang, 26300, Gambang, Kuantan, Pahang, Malaysia
e-mail: mrkhancep@yahoo.com

fiber is not fully materialized in robust structural applications for the aforesaid weaknesses. If these weaknesses of EFB fiber can be eliminated through surface modifications, then it can be possible to promote their resourceful uses [7–9].

Basically, the incompatibility between natural fiber and metallic nanofillers has appeared to be a great challenge in incorporating them into the fibers. Improvement in mechanical performances of natural fiber by nanofiller was attained by fiber surface modification with functionalized Cu nanoparticles [5]. The functional nanoparticles were obtained by synthesizing them in the presence of the hydrophilic polyvinyl alcohol (PVA) that surrounds them. However, this functionalization results in the partially negative charge environment around CuNPs for which they are not readily adsorbed on to the hydroxyl group containing fiber surfaces. To overcome this drawback, fiber surfaces are necessary to modify using a cationic agent before impregnating CuNPs. In this respect, a recent study on copper nanoparticles-coated fiber surfaces that revealed a good antimicrobial activity and suitably served in medical requirements is very noteworthy [10]. Till to date, no work about CuNPs incorporation in EFB fiber has been done by any other researcher for improving its mechanical performance. Therefore, the present work has been undertaken to modify the EFB fibers by CuNPs for exploiting them in due applications, especially in the area of natural fiber-reinforced nanocomposites where strong natural fibers are used as important fillers. With this view, EFB fibers were treated by 3-chloro-2-hydroxypropyltrimethyl ammonium chloride (cationic agent) with catalytic amount of sodium hydroxide and then the treated fibers were readily used for CuNPs incorporation.

On the other hand, natural fibers generally exhibit a high disparity of mechanical properties in a wide range of diameters even in the same bunch of fibers. To analyze this disparity in mechanical properties, the use of Griffith model can be notable [11]. Nonetheless, a two-parameter Weibull distribution model reportedly demonstrated in the least biased mechanical performances [5, 11–13]. Fiber strength is a statistical parameter which cannot be completely describable by a single value like many other common physical parameters such as fiber length, aspect ratio, mass, density, shape, etc. To describe the variability in strength of this material, preferably used statistical tool is the Weibull distribution that can satisfactorily indicate the homogeneity of the material and predict about the characteristic mechanical parameters of a material. To the best of our knowledge, this statistical model has not yet been applied to characterize the mechanical strength and modulus of any nanofiller reinforced EFB fibers.

In the present work, the mechanical properties of the EFB fibers were improved by surface modification with CuNPs and characterized by FTIR and FESEM. The observed mechanical performances of untreated and CuNPs impregnated EFB fibers were assessed by the Griffith and Weibull models. Thereafter, the weak-link model has been used for predicting the mechanical properties of the same fibers.

Experimental

Materials

Raw EFB fibers were collected from the LKPP Corporation Sdn. Bhd., Kuantan, Malaysia. A solution of 3-chloro-2-hydroxypropyltrimethyl ammonium chloride (CHPTAC) was purchased from Sigma-Aldrich. The raw fibers of an average diameter of 0.174 ± 0.073 mm were washed by water and dried under sunlight for 3 days. The fibers thus obtained are referred to untreated EFB (UEFB) fibers.

Synthesis of CuNPs

Sol of copper nanoparticles was synthesized in the polyvinyl alcohol system by the chemical reduction method and the procedure of synthesis was achieved from our previous work [14].

Cationization of UEFB fibers

The UEFB fibers were dipped in 36 % CHPTAC solution for cationization reaction at a constant temperature of 60 °C. Thereafter, 15 % sodium hydroxide with respect to the fiber-weight was added to the mixture and stirred for 15 min. The cationized EFB (CEFB) fiberswere rinsed with water and dried at the ambient conditions. The CEFB fibers were kept in the nano copper sol (214 mg/L) for 12 h to adsorb CuNPs. The CuNPs reinforced CEFB fibers abbreviated as treated EFB (TEFB) fibers were thus obtained.

Characterization

Transmission electron microscopy (TEM) was performed by a LEO 912 AB EFTEM operating at 120 kV to monitor the size of nanoparticles. A small drop of the liquid sol was placed over a carbon-coated microscopic copper grid (200 mesh size) and dried under vacuum at room temperature before measurements. Attenuated total reflectance (ATR) Fourier-transformed infrared (FTIR) spectra of UEFB, CEFB and TEFB fibers were recorded over the frequency range of 4,000–650 cm^{-1} using a Thermo Scientific Model Smart Performer attenuated total reflectance (ATR) accessory of Ge crystal, attached to a Thermo Scientific spectrophotometer (Model Nicolet Avatar-370) with a single bounce. The FTIR parameters were as follows: angle of incidence 45°, sampling area 2 mm; number of background scans, 32; number of scans, 32; optical resolution, 4.00 cm^{-1}. The single UEFB and TEFB fibers were subjected to the ASTM D3379-75 standard test method for measuring tensile strength and Young's modulus. The single fibers were individually placed in the grips of a DIA-STRON LTD/UK (FDAS 765) tensile testing machine with a gauge length of 10 and 50 mm. The fibers were stretched to failure at a rate of 3 mm/min using a 100 N-load cell. Strength and modulus were obtained using the diameters of individual fibers and the average value was calculated from the collected data of 100 fibers. Surface morphologies of UEFB,

CEFB and TEFB fibers were also investigated using a field emission scanning electron microscope (FE-SEM) of JEOL JSM-7600F, USA, equipped with an energy dispersive X-ray (EDX) system (OXFORD INCA. Fibers were mounted on sample holders with carbon tape and sputtered by platinum.

Thermal measurements of the samples were done by a thermogravimetric analyzer (TGA) (TA Instrument, Q500 V6.4, Germany) in a platinum crucible under nitrogen atmosphere (flow rate 40–60 mL/min) with a heating rate of 10 °C/min in the temperature range of 30–600 °C.

Results and discussion

CuNPs morphology

The TEM of the CuNPs is presented in Fig. 1. It can be seen that the particles are of spherical shape. From analysis of 100–500 nanoparticles of various diameters within the range of 1.0–10.5 nm, the average particle size was determined as 3.5 ± 1.1 nm. The CuNPs from the sol were further impregnated onto the fibers.

FTIR analysis of different EFB fibers

The ATR-FTIR spectra of different EFB fibers are displayed in Fig. 2a, b. The important peaks are attributed to the O–H stretching at 3,450–3,300 cm^{-1}, the C–H stretching at 2,926 cm^{-1}, and the C–H bending (wagging) at 1,318 cm^{-1} by others [15]. The absorbance frequency of UEFB fiber (Fig. 2a(i)) at 1,740 cm^{-1} indicates

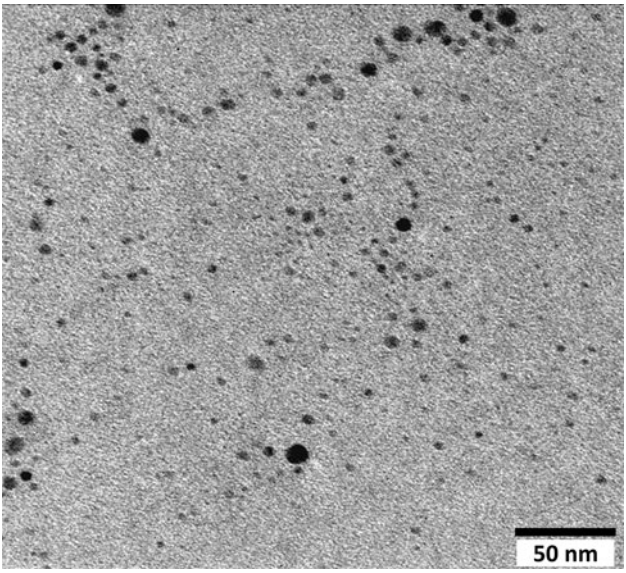

Fig. 1 TEM image of CuNPs sol

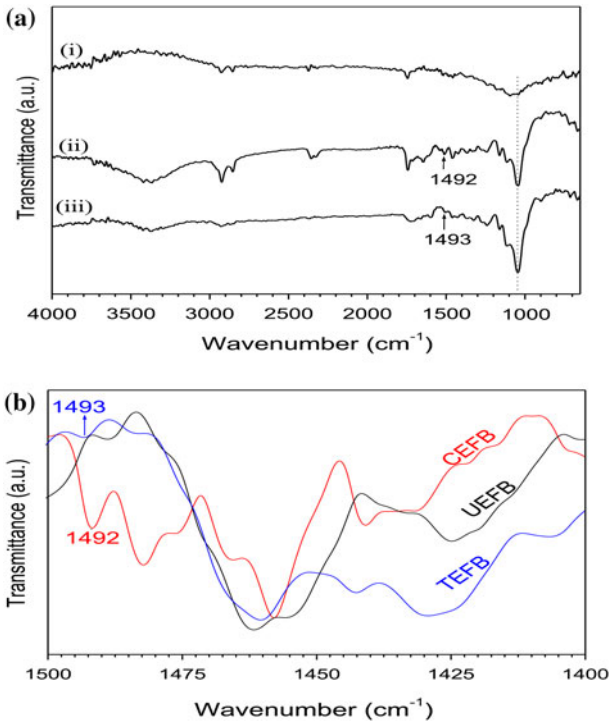

Fig. 2 FTIR spectra of **a** UEFB (*i*), CEFB (*ii*), and TEFB (*iii*) fibers, and **b** extended form at 1,500–1,400 cm^{-1} for the same fibers

the stretching vibration of carbonyl groups of hemicellulose and lignin [5, 16]. Careful observation shows that the new peaks at 1,492 cm^{-1} (Fig. 2a(ii), b) and 1,493 cm^{-1} (Fig. 2a(iii), b), respectively, appear in the FTIR spectra of CEFB and TEFB, but not found in the spectrum of UEFB fiber (Fig. 2a(i), b). Comparative analysis from the maximum intensities of absorption frequency at 1,648 cm^{-1} (absorption band related to the cellulose fibers) and 1,495 cm^{-1} (characteristic absorption frequency of cationic agent attached to the fiber) reveals $\sim$39 % cationization of fibers [15], ensuring the cationization process. Besides, the difference in the absorption pattern at around 1,495 cm^{-1} for CEFB and TEFB fibers may indicate the incorporation of CuNPs in the fibers. Moreover, the appearance of the clearly visible sharp peak in the spectra of CEFB and TEFB at 1,048 cm^{-1} may correspond to the stretching frequency of carbon–nitrogen (C–N) single bond, which is absent in the spectrum of UEFB. This group may come from the cationic agent.

Morphology of CuNPs impregnated and un-impregnated fibers and their TGA

Figure 3a–c represents the FESEM micrographs of UEFB, CEFB and TEFB fibers, respectively. The apparent changes in surface structure of CEFB fibers from UEFB

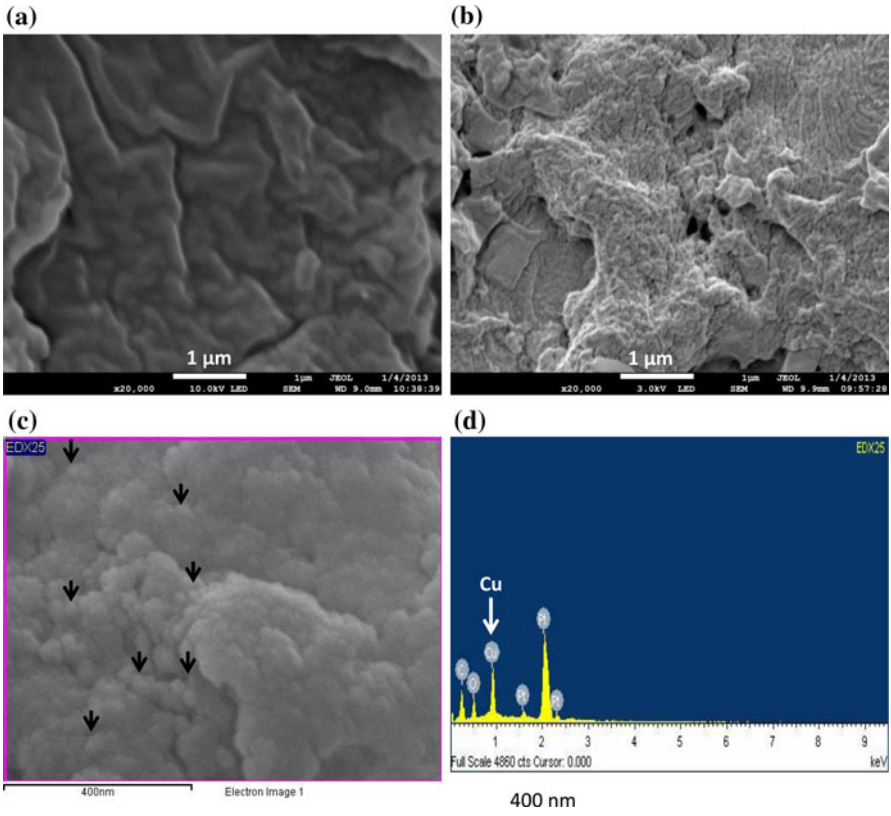

Fig. 3 FESEM images of **a** UEFB and **b** CEFB. Electron image of TEFB (**c**) and EDX spectrum (**d**) taken from (**c**)

fibers indicate the adhesion of cationic agent to the fiber surface. CuNPs incorporation is obvious in the micrographs of TEFB fiber (shown by arrows). The EDX spectrum collected from the entire region of Fig. 3c is illustrated in Fig. 3d, confirming a considerable amount of CuNPs incorporation into the fibers. In fact, EFB fibers and other natural fibers contain major some elements such as carbon (C) and oxygen (O) [17, 18]. The initial high peaks were attributed by carbon and oxygen. Another high peak at about 2.1 keV was originated from platinum (Pt), which was used for sputtering. Moreover, from FTIR analysis, ~39 % cationization of fiber was noticed; this result and the FESEM images were confirmed that CHPTAC was attached on the fiber surface non-homogenously. Consequently, CuNPs were attached only with those points of fibers where CHPTAC moieties existed. Furthermore, considering ten FESEM images and EDX spectra, 5–18 % of CuNPs incorporation was noticed on the TEFB fiber surfaces. Figure 4 depicts the TGA thermograms for UEFB and TEFB fibers. The degradation temperatures at 50 % weight-loss for UEFB and TEFB fibers are analyzed to be 347 and 339 °C, respectively. It is found that at 600 °C, the residue content for TEFB fiber is 17.6 % and that for UEFB fiber is 15.4 %, showing higher residues for TEFB fibers. These

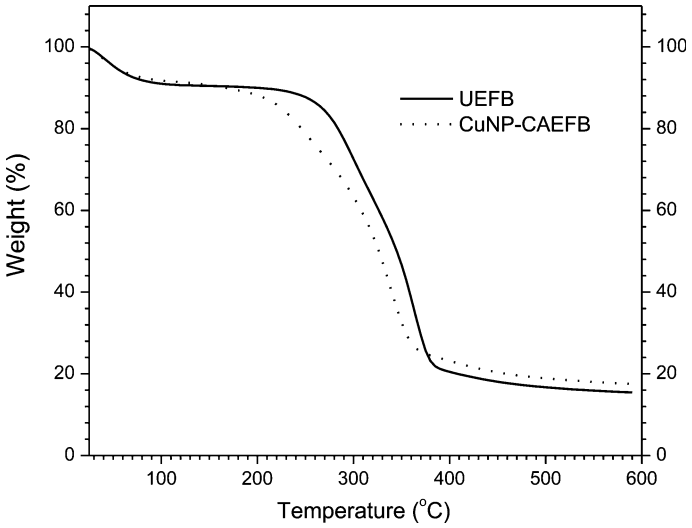

Fig. 4 TGA thermograms of UEFB and TEFB fibers

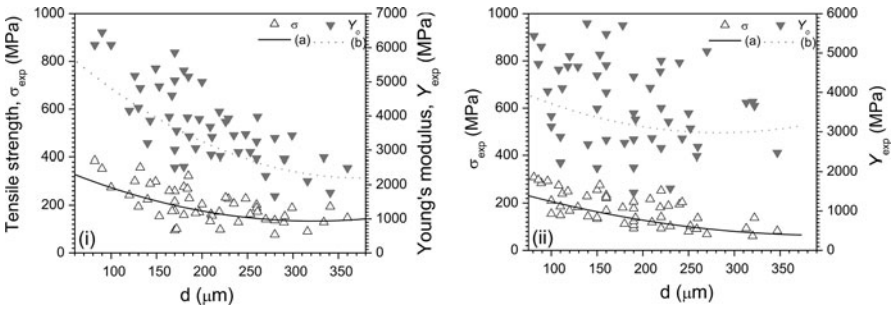

Fig. 5 Tensile strength/modulus versus diameter plots: for fibers of lengths **i** 10, **ii** 50 mm. *Open triangle* and *filled inverted triangle* are observed values; *a* and *b* indicate the Griffith plots

results, in addition to surface morphological outcomes, demonstrate the incorporation of CuNPs in EFB fibers.

Mechanical performances of different EFB fibers

Tensile strength (σ) and Young's modulus (Y) as a function fiber diameter (d) for UEFB fibers of length 10 and 50 mm are depicted in Fig. 5i(a), (b), ii(a), (b), respectively. The incorporated nanoparticles in natural fibers can increase the mechanical strength of the fibers [5, 19]. However, the apparent scatter can be related to test parameters, plant characteristics and area measurements, and therefore, calls for use of models to evaluate their mechanical properties. The following Griffith empirical expression is used to model the variation in mechanical properties with fiber diameter [11]: $x(d) = A + B/d$, where $x(d)$ represents either σ

Table 1 Parameters for the Griffith and Weibull distribution models obtained from UEFB and TEFB fibers of different lengths

Fibers	Length (mm)	Griffith model				Weibull distribution model			
		A (MPa) for TS	B (MPa-μm) for TS	A (MPa) for YM	B (MPa-μm) for YM	σ_0 (MPa)	Y_0 (MPa)	m for TS	m for YM
UEFB	10	65.6	24,992	1,454	428,333	225	4,099	3.116	3.808
	50	55.2	19,122	2,808	144,795	200	3,988	2.721	3.821
TEFB	10	98	26,602	1,846	478,005	269	4,506	3.147	3.895
	50	72	22,027	3,070	276,222	242	4,309	3.035	3.876

or Y, and A and B are two model parameters. The superimposed lines are drawn by the Griffith model, revealing a decrease in fiber strength/modulus as the d increases. The probability of having a large number of flaws was found in a fiber with a large cross-sectional area as compared to a fiber with a small cross-sectional area [11]. Hence the observed low strength/modulus for fiber of a large d than a fiber of a small d is rational. The values of model parameters obtained for fibers of lengths 10 and 50 mm are reported in Table 1. Due to a notable divergence of the curve from the experimental values, the Griffith model cannot be used to accurately interpolate the observed results. For this reason, another two-parameter model, namely the Weibull distribution, has been applied to define the fiber strength/modulus. For a mechanical study, if a fiber has the length L, then the probability of its failure at a stress x can be expressed by the following term [5, 11–13]: $F(x) = 1 - \exp\left[-L(x/x_0)^m\right]$, where, x_0 is the characteristic strength or modulus (σ_0 or Y_0) of the fiber and m the Weibull modulus. For measuring $F(x)$ values, the following estimator was used: $F(i(x)) = i(x)/(n+1)$, where, i is the rank of the ith data and n the total number of data. Using the above relation of $F(x)$, the value $x_{0(1)}$ obtained for a length L_1 may be used to predict the value $x_{0(2)}$ for a length L_2 by means of the following weak-link scaling (WLS) formula [12]: $x_{0(2)} = x_{0(1)}(L_1/L_2)^{m^{-1}}$. Figures 6a, b and c, d show the Weibull plots for UEFB and TEFB fibers, respectively, and the lengths of 10 and 50 mm, respectively. The experimental data points demonstrate a good fit using the Weibull distribution. The Weibull parameters (σ_0, Y_0 and m) obtained from the Weibull plots for the two different lengths of both treated and untreated fibers are summarized in Table 1. The fiber of small length reveals a high Weibull modulus, as also noted elsewhere [12, 13]. The observed parameters for the fibers show an expected trend that a short-length fiber contributes to a high strength/modulus. Analyses indicate a discrepancy between observed average σ_{ave} (or Y_{ave}) and calculated σ_0 (or Y_0) values of about 11 %, which can be a reasonably accepted value. Using WLS relation, the value of σ_0 predicted for the fiber length of 50 mm from the fiber length of 10 mm is 134 MPa. This gives a deviation of about 33 % from the characteristic strength of 200 MPa of 50-mm length fiber with a reasonable agreement as assessed by other [12]. Interestingly, TEFB fibers also show the same deviation. The results indicate a

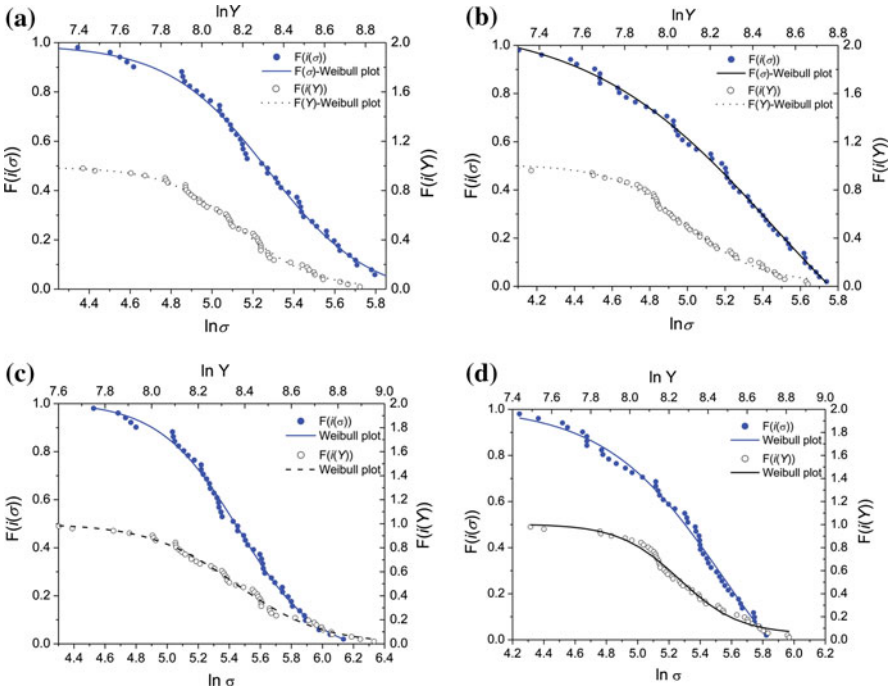

Fig. 6 The probability of failure versus lnσ or lnY plots of lengths **a** 10, **b** 50 mm for UEFB fibers, and **c** 10, **d** 50 mm for TEFB fibers. *Open circle* and *filled circle* are from estimators and *straight line* and *dashed line* are the Weibull plots

Table 2 Increment of tensile strength of different natural fibers due to the treatment at room temperature

Fiber	Length (mm)	Treatment		TS increment (%)	Reference
		Condition	Duration		
Coir	10	6 wt% Alkali	4 weeks	22	[20]
EFB	50	2 wt% Alkali	30 min	23	[21]
Kenaf	3.5	7 wt% Alkali	6 h	12	[22]
EFB	10	0.0214 wt% CuNPs	12 h	20	Present work

significant improvement in σ_0 by 20 % for the 10-mm length fiber and by 21 % for the 50-mm length fiber after Cu nanoparticle incorporation. This increase in tensile strength for TEFB fibers is relatively higher as compared to other fibers shown in Table 2 [20–22]. However, the discrepancy in the trends of the Weibull modulus for YM observed for UEFB and TEFB fibers of different lengths is due to reason that the probability of having a large number of flaws in a fiber for a long length is higher than that in a fiber for a short length [11]. Hence the observed low strength/modulus for fiber of a large L than a fiber of a small L is rational.

Conclusion

Easily degradable and poor mechanical property possessing EFB fibers are tailored by CuNPs through CHPTAC. In CEFB and TEFB fibers, significant number of CHPTAC and CuNPs incorporation is noticed, respectively. Mechanical properties (tensile strength and modulus) of EFB fibers have been assessed by single fiber tensile tests and the results are improved by CuNPs incorporation. These results are analyzed through Griffith model and a two-parameter Weibull distribution. Griffith model provides high scattering information of mechanical properties. Weibull distribution function reveals a good fit with the observed data and a good scaling to strength/modulus of single fiber at different lengths. Improvements in fibers strength/modulus are achieved due to the improved fiber–filler interfacial bonding, as demonstrated by FESEM, EDX and FTIR analyses. The results of the mechanical properties confirm that this strong fiber can show some potential as reinforcement in polymer matrix composites.

Acknowledgments The authors would like to acknowledge Universiti Malaysia Pahang (UMP), Malaysia, for funding of this work under the grant number of GRS 110322.

References

1. Klemm D, Kramer F, Moritz S, Lindström T, Ankerfors M, Gray D et al (2011) Nanocelluloses: a new family of nature-based materials. Angew Chem Int Ed 50:5438–5466
2. Weng Z, Su Y, Wang DW, Li F, Du JH, Cheng HM (2011) Graphene–cellulose paper flexible supercapacitors. Adv Energy Mater 1:917–922
3. Tsioptsias C, Panayiotou C (2008) Preparation of cellulose-nanohydroxyapatite composite scaffolds from ionic liquid solutions. Carbohydr Polym 74:99–105
4. Ahmad EEM, Luyt AS, Djokovic V (2013) Thermal and dynamic mechanical properties of bio-based poly(furfuryl alcohol)/sisal whiskers nanocomposites. Polym Bull 70:1265–1276
5. Chowdhury MNK, Beg MDH, Khan MR, Mina MF (2013) Modification of oil palm empty fruit bunch fibers by nanoparticle incorporation and alkali treatment. Cellulose 20:1477–1490
6. Law KN, Daud WRW, Ghazali A (2007) Morphological and chemical nature of fiber strands of oil palm empty-fruit bunch (OPEFB). BioResources 2:351–362
7. Sousa MV, Montero SN, d'Almeid JRM (2004) Evaluation of pre-treatment, size and molding pressure on flexural mechanical behavior of chopped bagasse–polyester composites. Polym Test 23:253–258
8. Hoareau W, Tradade WG, Siegmund B, Castellan A, Frollini E (2004) Sugarcane bagasse and curaua lignins oxidized by chlorine dioxide and reacted with furfuryl alcohol: characterization and stability. Polym Degrad Stab 86:567–576
9. Abdul Khalil HPS, Poh BT, Issam AM, Jawaid M, Ridzuan R (2010) Recycled polypropylene-oil palm biomass: the effect on mechanical and physical properties. J Reinf Plast Compos 29:1117–1130
10. Raffi M, Mehrwan S, Bhatti TM, Akhter JI, Hameed A, Yawar W, ulHasan MM (2010) Investigations into the antibacterial behavior of copper nanoparticles against *Escherichia coli*. Ann Microbiol 60:75–80
11. Rosa IM, Kenny JM, Puglia D, Santulli C, Sarasini F (2010) Morphological, thermal and mechanical characterization of okra (*Abelmoschus esculentus*) fibers as potential reinforcement in polymer composites. Compos Sci Technol 70:116–122
12. Pickering KL, Beckermann GW, Alam SN, Foreman NJ (2007) Optimising industrial hemp fiber for composites. Compos Part A 38:461–468
13. Roy A, Chakraborty S, Kundu SP, Basak RK, Majumder SB, Adhikari B (2012) Improvement in mechanical properties of jute fibres through mild alkali treatment as demonstrated by utilisation of the Weibull distribution model. Bioresour Technol 107:222–228

14. Chowdhury MNK, Beg MDH, Khan MR, Mina MF (2013) Synthesis of copper nanoparticles and their antimicrobial performances in natural fibres. Mater Lett 98:26–29
15. Khalil-Abad MS, Yazdanshenas ME, Nateghi MR (2009) Effect of cationization on adsorption of silver nanoparticles on cotton surfaces and its antibacterial activity. Cellulose 16:1147–1157
16. Chowdhury MNK, Khan MW, Mina MF, Beg MDH, Khan MR, Alam AKMM (2012) Synthesis and characterization of radiation grafted films for removal of arsenic and some heavy metals from contaminated water. Radiat Phys Chem 81:1606–1611
17. Nazir MS, Wahjoedi BA, Yussof AW, Abdullah MA (2013) Eco-friendly extraction and characterization of cellulose from empty fruit bunches. BioResources 8:2161–2172
18. Sivaraja M, Kandasamy, Velmani N, Pillai MS (2010) Study on durability of natural fibre concrete composites using mechanical strength and microstructural properties. Bull Mater Sci 33:719–729
19. Chattopadhyay DP, Patel BH (2009) Improvement of physical and dyeing properties of natural fibers through pre-treatment with silver nanoparticles. Ind J Fiber Text Res 34:368–373
20. Gu H (2009) Tensile behaviours of the coir fibre and related composites after NaOH treatment. Mater Des 30:3931–3934
21. Norul Izani MA, Paridah MT, Anwar UMK, Mohd Nor MY, H'ng PS (2013) Effects of fiber treatment on morphology, tensile and thermogravimetric analysis of oil palm empty fruit bunches fibers. Compos Part B 45:1251–1257
22. Islam MR, Beg DH, Gupta A (2013) Characterization of alkali-treated Kenaf fibre-reinforced recycled polypropylene composites. J Thermoplast Compos Mater. doi:10.1177/0892705712461511